electronics

Article

Investigation of Contact Surface Changes and Sensor Response of a Pressure-Sensitive Conductive Elastomer

Takeru Katagiri [1,*], Nguyen Chi Trung Ngo [1], Yuki Togawa [2], Sogo Kodama [2], Kotaro Kawahara [3], Kazuki Umemoto [2], Takanori Miyoshi [4] and Tadachika Nakayama [1]

[1] Department of Science of Technology Innovation, Nagaoka University of Technology, 1603-1 Kamitomioka, Nagaoka, Niigata 940-2188, Japan
[2] Department of Mechanical Engineering, Nagaoka University of Technology, 1603-1 Kamitomioka, Nagaoka, Niigata 940-2188, Japan
[3] INABA RUBBER Co., Ltd., 3-3-15 Kyomachibori, Nishi, Osaka, Osaka 550-0003, Japan
[4] Department of System Safety, Nagaoka University of Technology, 1603-1 Kamitomioka, Nagaoka, Niigata 940-2188, Japan
* Correspondence: s195003@stn.nagaokaut.ac.jp

Abstract: The pressure-sensing mechanisms of conductive elastomers, such as conductive networks, and tunneling effects within them have been extensively studied. However, it has become apparent that external pressure can significantly impact the contact area of polymeric materials. In this study, we will employ a commercially available conductive elastomer to investigate changes in resistance and contact surface under external pressure. Resistance measurements will be taken with and without applying conductive grease to the surface of the elastomer. This allows us to observe changes in resistance values associated with pressure variations. Furthermore, as pressure is applied to the conductive elastomer, the contact area ratio increases. Such an increase in the contact area and its correlation to changes in conductance values will be assessed.

Keywords: conductive elastomer; conductive rubber; pressure sensor; piezoresistive sensor; elastomer; composite

check for updates

Citation: Katagiri, T.; Ngo, N.C.T.; Togawa, Y.; Kodama, S.; Kawahara, K.; Umemoto, K.; Miyoshi, T.; Nakayama, T. Investigation of Contact Surface Changes and Sensor Response of a Pressure-Sensitive Conductive Elastomer. *Electronics* **2023**, *12*, 4532. https://doi.org/10.3390/electronics12214532

Academic Editor: Francesco Giuseppe Della Corte

Received: 4 October 2023
Revised: 30 October 2023
Accepted: 2 November 2023
Published: 3 November 2023

1. Introduction

Force sensors with piezoelectric behavior can be classified into those with capacitance [1–6] and those with piezoelectric resistance. Flexible elastomer composite sensors, which include conductive fillers in polymeric materials, have been proposed for elastomers with piezoelectric resistance. External mechanical forces and strains can be detected using these composites as sensors. Recently, several studies have been conducted on composites with multifunctionality and sustainability, such as those with self-healing properties [7] and those that use plant fibers as fillers [8]. Regarding the conductive mechanism in polymer materials containing conductive fillers, in addition to the structures of conductive particles inside the composite [9] and the electric field generated between carbon particles [10], it is considered that electric current flows owing to electrons jumping over an insulating film, commonly known as the tunneling effect [11,12]. In the development of piezoresistive composite sensors whose main components are polymeric materials, many researchers have previously argued that resistance changes are caused by changes in the conductive network inside the composite material [13–20]. However, there are studies focusing on the contact between conductive elastomers and electrodes. There is a report that the pressure-sensitive characteristics of polymeric materials with known volume resistivity can be changed by changing the shape of the elastomer surface [21]. Additionally, a report claimed that when pressure is applied to a conductive elastomer, the contact area between the elastomer and the electrode increases, and that only the change in the contact area determines the resistance value that occurs between the conductive elastomer and the electrode [22]. Furthermore, some reports suggest that both internal changes in the elastomer and changes in the contact surface of the elastomer affect sensor response [23–26]. Nevertheless, to the best of our knowledge, there has been no report in which an elastomer's surface was coated with conductive paste, pressure was applied while the elastomer was in a stable electrical contact condition, and an internal resistance value change was verified. As well conductive elastomers, it has been confirmed that when rubbers and elastomers come into contact, they form a multi-contact interface rather than a single apparent area. Likewise, it has been observed that the contact area of this interface increases as pressure is applied after the objects have initially made contact [27–29]. Based on these previous studies, it was thought that even in commercially available conductive elastomers, changes inside the composite, changes on the composite surface, or both changes are captured as a sensor response.

Previous research using commercially available conductive elastomers includes the development of wide-area mapping sensors [19] and examples of their use as sensors for machine learning [20,30]. Pressure-sensitive sensors using polymeric materials and conductive fillers must consider characteristics such as hysteresis [13], resistance change under constant load [20,31], and recovery time [32], while, by combining elastomer with electrodes, it is possible to easily apply pressure-sensitive functions as a pressure-sensitive sensor. Furthermore, because it can be attached to curved surfaces, it is also used as a pressure-sensitive sensor [33] and a slip sensor [34,35]. Based on this result, it can be said that conductive elastomer sensors are highly compatible with machine learning and robots. If changes in the contact surface of a commercially available conductive elastomer affect the sensor response, the contact condition must be considered. Moreover, this is necessary for selecting electrodes to be used with the conductive elastomer and for determining the conditions for using the conductive elastomer as a force sensor for machine learning or robots. However, in the studies using commercially available conductive elastomers, there have been no reports that consider changes in contact between the elastomer and electrodes, and the changes in the insulation properties and sensor response of conductive elastomers are thought to be due to the conductive network inside the elastomer [19,34].

Therefore, in this study, we investigate changes in the resistance value of conductive elastomers and changes in the contact surface and consider the effects of changes in internal resistance and contact area on sensor response. In this study, we first presented the filler material contained in the conductive elastomer and observed the material properties to confirm the distribution of the filler in the conductive elastomer. Additionally, we obtained the sensor response when conductive grease was applied to the surface of the conductive elastomer and measured the resistance change inside the conductive elastomer. Furthermore, we measured changes in the contact surface due to external pressure, and based on these results, we report on the possibility that changes in the contact surface are influencing the sensor's response.

2. Materials and Methods

2.1. Material Selection

The conductive elastomer composite (INABA RUBBER Co., Ltd., Osaka, Japan, high-sensitivity sheet) used in this study is shown in Figure 1. This elastomer can be used as a pressure-sensitive sensor when placed on an electrode. The material has extremely high resistance when no load is applied, but resistance decreases with increasing pressure. This high resistance makes it difficult to confirm conductivity. Moreover, it shows electrical characteristics in which resistance decreases with increasing pressure [34].

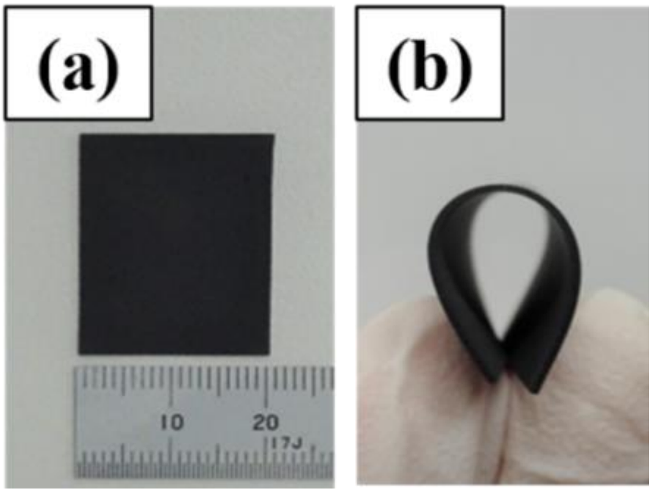

Figure 1. Digital photograph of the elastomer film: (**a**) surface in contact with the electrode (width 20 mm × vertical width 30 mm); (**b**) bendable elastomer film (thickness 0.5 mm).

Table 1 shows the volume resistivity, average particle diameter, and average fiber length of the materials used in this conductive elastomer, which were disclosed by the manufacturer of this conductive elastomer, and the filler materials investigated by the filler material manufacturer.

Table 1. Properties of materials used for the conductive elastomer composite.

Material	Volume Resistivity (Ω·cm)	Mean Particle Size (μm)	Mean Fiber Length (μm)
Liquid silicone rubber (PDMS)	5×10^{15}	-	-
Carbon particle	2.1×10^{-2}	34×10^{-3}	-
Aluminum oxide particle	-	-	-
Silicone elastomer powders	-	3	-
Silicone resin powders ($RSiO_3/2$)	-	20	-
DENTALL ($K_2O{\cdot}6TiO_2/SnO_2$)	10	-	10–20

Silicone rubber (Shin-Etsu Chemical Co., Ltd., Tokyo, Japan: KE-445) was used as a binder in this conductive elastomer composite, and conductive microfibers with a ceramic conductive coating on potassium titanate fibers (DENTALL, Otsuka Chemical Co., Ltd., Osaka, Japan: WK-200B) and carbon nanoparticles (Lion Specialty Chemicals Co., Ltd., Tokyo, Japan: EC600JD) were used as highly conductive fillers.

In addition to highly insulating silicone materials such as spherical silicone elastomer powder (Dow Toray Co., Ltd., Tokyo, Japan: EP-5500) and irregularly shaped silicone resin powder (NIKKO RICA Co., Ltd., Tokyo, Japan: MSP-150), alumina particles (ASAHI CHEMICAL INDUSTRY Co., Ltd., Tokyo, Japan: L20N2-F1210) were used.

To clarify how these fillers are distributed in this conductive elastomer, surface and cross-sectional observations were performed using a scanning electron microscope (SEM; Hitachi High-Tech Corporation: FlexSEM 1000 II). In addition, elemental mapping images were obtained for the cross-section of the conductive elastomer using Energy-dispersive X-ray spectroscopy (Oxford Instruments Holdings 2013 Inc., Belfast, UK), and the state of dispersion of the filler used in this conductive elastomer was observed.

2.2. Determination of Resistance Change in the Elastomer

A pressure test was conducted with conductive grease, providing stable electrical contact between the conductive elastomer and the electrode. In addition, the change in resistance value of the conductive elastomer obtained with and without conductive grease was compared. The change in resistance value against the pressure is obtained using a pressure tester (INABA RUBBER Co., Ltd.: F-R testing machine) shown in Figure 2a. Figure 2b shows a schematic diagram of the tip of the pressure testing machine. The shape of the contact surface of the indenter that compresses the conductive elastomer is 6 mm × 6 mm. For a 20 mm × 30 mm conductive elastomer placed on a copper substrate. When conductive grease is not used, the indenter moves from a non-contact position and applies pressure in a direction perpendicular to the elastomer at a speed of 200 cm/min. At this time, the pressure was calculated from the apparent contact area of the indenter (36 mm^2), and the pressure was increased to 550 kPa. After the maximum load is reached, the indenter moves at a speed of 200 cm/s in the upward direction to release the applied pressure. The elastomer and indenter eventually return to their non-contact state. By moving the indenter up and down once, the resistance value changes during pressurization and depressurization processes can be obtained. The minimum pressure for the measured resistance value is 11 kPa because the resistance value measurement is started in a non-contact state when conductive grease is not used. Figure 2c shows the test situation when conductive grease (NIKKO SHOJI Co., Ltd., Shizuoka, Japan: IF-20) was used. The surface in contact with the conductive elastomer and the intender was masked to a size of 6 × 6 mm as much as possible, and conductive grease was applied to that surface with a cotton swab. Conductive grease is applied to the bottom of the elastomer within a range of 15 × 15 mm. A thin layer of conductive grease, weighing approximately 0.1 g in total, is applied to the elastomer. Increased conductive grease application will cause the conductive grease to spread out over the top of the elastomer and beyond the indenter's shape when pressed by the indenter. Because spilling-over grease might result in wrong measurements of resistance values, one should be extremely cautious about the over-application so that the covering area of the conductive grease does not extend over the area of the indenter. It is interesting to note that, in our study, when the conductive grease is applied, the resistance value of the elastomer is measurable, even when the applied pressure is zero. This is not possible with other existing research that does not use the conductive grease; that is, the resistance value at zero pressure is too large to be considered a valid measurement. A maximum pressure of 550 kPa is applied using an indenter, even with conductive grease. The pressure is then reduced and ultimately returns to a non-contact state. The conductive grease used in this test had a volume resistivity of 150 Ω·cm at 25 °C, and the test was conducted while keeping the room temperature at 25 °C.

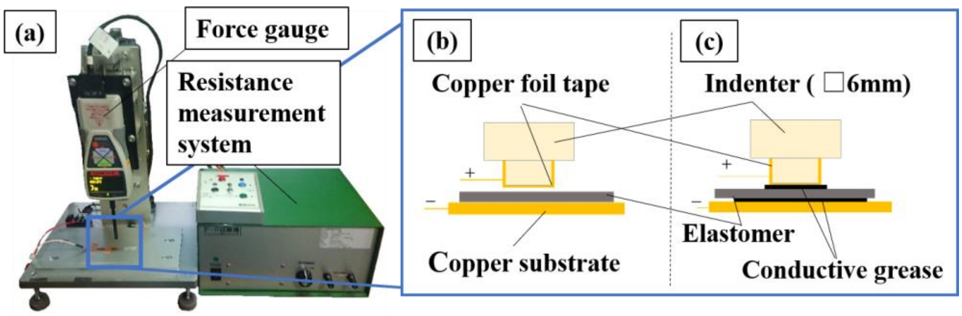

Figure 2. Configuration of the pressure tester: (**a**) photograph of the pressure tester; (**b**) structure of the test tip of the pressure tester; (**c**) test situation when conductive grease is used.

2.3. Acquisition Method of Contact Area Variation

In order to investigate the rate of change in the contact area of the conductive elastomer with respect to pressure, we created a compressed surface observation apparatus shown in

Figure 3. In this apparatus, a load cell (TEAC Corporation, Tokyo, Japan: TC-FSRSP(T)50N-G3) is installed on the *z*-axis stage (SIGMAKOKI Co., Ltd., Tokyo, Japan: TSD-603WP), and a force is applied to the elastomer. As shown in Figure 3b, this elastomer is sandwiched between glasses. The change in the contact area between the glass and elastomer was observed using a confocal microscope (Lasertec Corporation, Yokohama, Japan: OPTELICS H1200). The conductive elastomer was cut out into a circular shape with a diameter of 3 mm, and the shape of the contact with the glass was specified. At this time, external pressure is applied in 100 kPa increments from 0 to 600 kPa at a pressure calculated from the apparent area of the conductive elastomer (7.06 mm^2). A lens with a minimum magnification of 10× in this confocal microscope was used to obtain the widest image of the elastomer surface. As shown in Figure 3c, the field-of-view of the lens was 1.78 mm × 1.78 mm. The image captured at this time was binarized, and the contact area of the elastomer with the glass was measured. The tests were performed in a yellow room where the room temperature was maintained at 25 °C and was not affected by sunlight. To process the images obtained via confocal microscopy, the same contrast and binarization threshold values were used throughout the experiment.

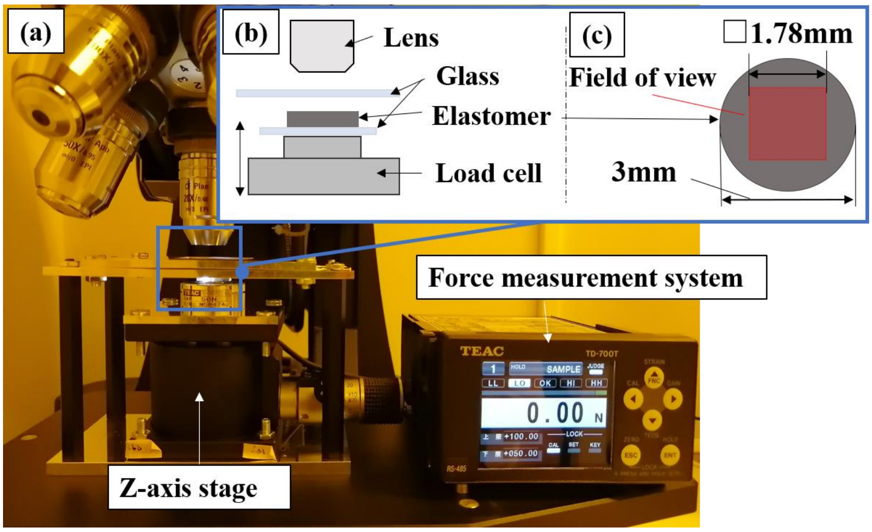

Figure 3. Compression surface observation device and configuration diagram: (**a**) digital photograph of the compressed surface observation system; (**b**) schematic of the compressed part of the elastomer; (**c**) observation area of the elastomer.

3. Result and Discussion

3.1. Material Analysis

Figure 4 shows the results of observing the surface and cross-section of the conductive elastomer. Figure 4a,b show the SEM images of the conductive elastomer surface magnified 100 and 5000 times, respectively. In Figure 4a, an angular filler of approximately 20 μm can be seen from the surface layer, which is thought to be irregularly shaped silicone resin powder. Furthermore, in Figure 4b, spherical fillers and fibrous fillers can be confirmed. Figure 4c,d are images of the cross-section of the conductive elastomer magnified 100 times and 5000 times, respectively. In the cross-section, it was confirmed that spherical and fibrous fillers were distributed in the same way as those on the surface.

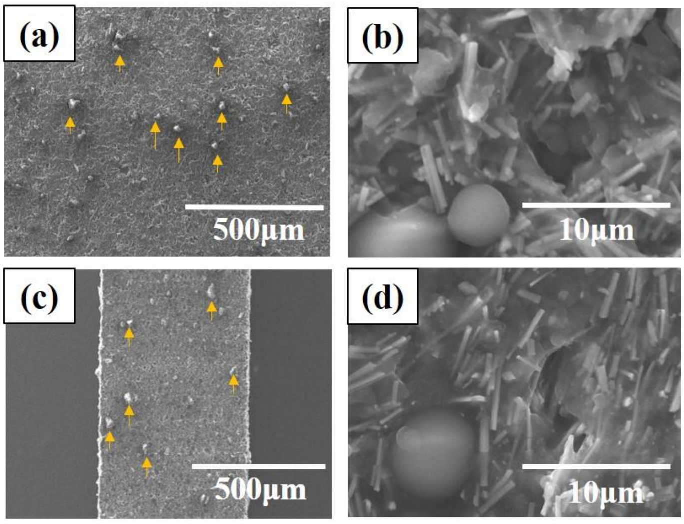

Figure 4. SEM images: (**a**,**b**) top view of the elastomer; (**c**,**d**) cross-sectional view of the elastomer (yellow arrows indicate amorphous silicone resin powder).

Figure 5a–h shows elemental mapping images based on SEM images. Figure 5a shows the conductive elastomer magnified 1000 times. In Figure 5a, the spherical filler is shown, and Si element was detected from the results in Figure 5b. Therefore, it can be seen that these spherical fillers are silicone elastomer powders. In Figure 5a, the silicone elastomer powder is distributed in an aggregated manner, and each silicone elastomer particle exists in an undispersed state. Furthermore, the fibrous filler is a titanium material, as shown in Figure 5c, and the elements Sn, K, and O associated with titanium materials can be confirmed by Figure 5d–f, indicating that these materials are DENTALL. The presence of Al and C is confirmed in Figure 5g,h, respectively. The carbon nanoparticles and alumina particles, which cannot be identified in the SEM images shown in Figure 4b,d are believed to be dispersed in the silicone rubber combined with the silicone elastomer powder and DENTALL. The results of SEM images and elemental mapping revealed that there was no particular difference in the distribution of filler on the surface and inside of this conductive elastomer, and that filler was distributed both on the surface and inside the conductive elastomer.

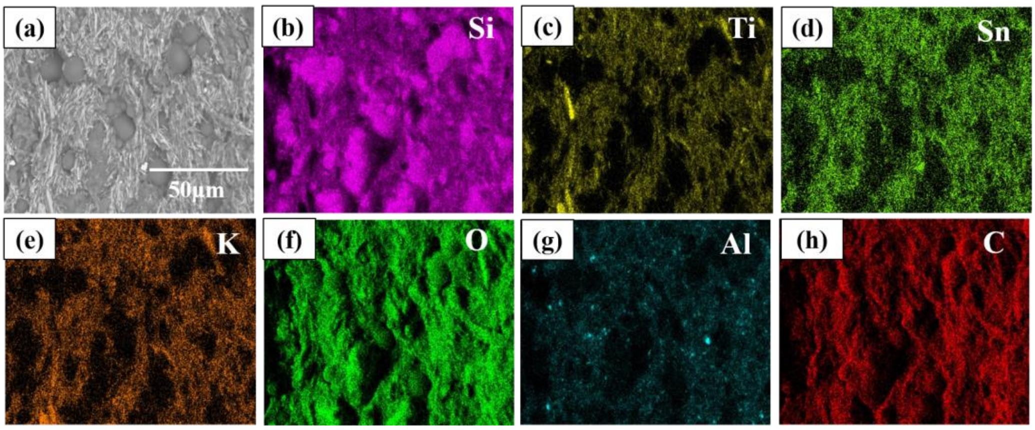

Figure 5. Elemental mapping images: (**a**) SEM image of the elastomer film; (**b**–**h**) elemental mapping images of Si, Ti, Sn, K, O, Al, and C elements corresponding to (**a**).

3.2. Comparison of Sensor Response by Pressure Test

Figure 6 shows the change in resistance value of the conductive elastomer against pressure when the pressure test was conducted five times, and the change in resistance value of the conductive elastomer against pressure when conductive grease was applied to the conductive elastomer. During the pressurization process, the pressure is increased from a minimum value of 11 kPa to a maximum value of 550 kPa. Moreover, the pressure of the depressurization process is reversed compared to that of the pressurization one. When the pressure was increased, the resistance value was 110 kΩ at an applied pressure of 11 kPa without applying conductive grease, and it was 1.1 kΩ when the maximum load of 550 kPa was applied. In contrast, when conductive grease was applied, the resistance value was 1.3 kΩ at an applied pressure of 11 kPa, and 57 Ω when a maximum load of 550 kPa was applied. Furthermore, when conductive grease was used, a resistance value of 3.1 kΩ was measured even when no load was applied. When calculating the resistance value, assuming that the thickness of the conductive grease applied to the conductive elastomer is 0.1 mm, the resistance value of the conductive grease generated on the surface of the conductive elastomer was 8.4 Ω. At this time, the resistance value of the conductive grease was less than 0.3% of the resistance value (3.1 kΩ) of the conductive elastomer measured under no load. Therefore, evidently, the resistance value obtained in a pressure test using conductive grease indicates the resistance value inside the conductive elastomer. These results revealed that the insulation during no-load conditions was not caused by the inside of the conductive elastomer. Additionally, a pressure test using conductive grease revealed that the resistance value inside the conductive elastomer decreased when external pressure was applied. When using conductive grease, the phenomenon in which the resistance value changes inside the conductive elastomer is thought to be due to changes in the conductive network inside the conductive elastomer, as described in previous research.

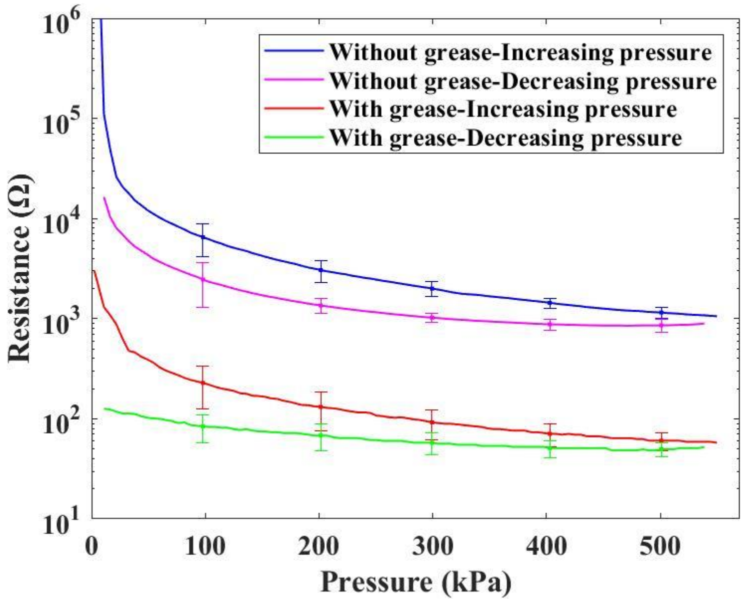

Figure 6. Resistance change of conductive elastomer (average value every 11 kPa and standard deviation every 100 kPa).

3.3. Percentage Change in Contact Area of Conductive Elastomer due to Compression

Figure 7 shows images taken during compression surface observation as pressure increases. As this conductive elastomer was black, the surface in contact with the glass absorbed light and was observed as a black pattern. It can be seen that this black pattern increases with the pressure applied to the conductive elastomer. Using this black pattern as the contact surface, Figure 8 shows the ratio of the contact surface to the increase in pressure: Ar/Ao (Ar: contact area, Ao: lens visual field area) when the test was conducted five times. The results showed that the contact area ratio increased nonlinearly as the pressure increased. When 100 kPa is applied to the conductive elastomer, it only accounts for 1.4% of the entire surface area of the conductive elastomer. In addition, the contact area increased with the increase in pressure, and when a pressure of 500 kPa was applied, it was 40.9% of the entire conductive elastomer. Also, the elastomer used in this compression surface observation has a shape diameter of 3 mm, and even under 600 kPa of compressive load, no dimensional deformation, such as expansion or change in diameter, was observed.

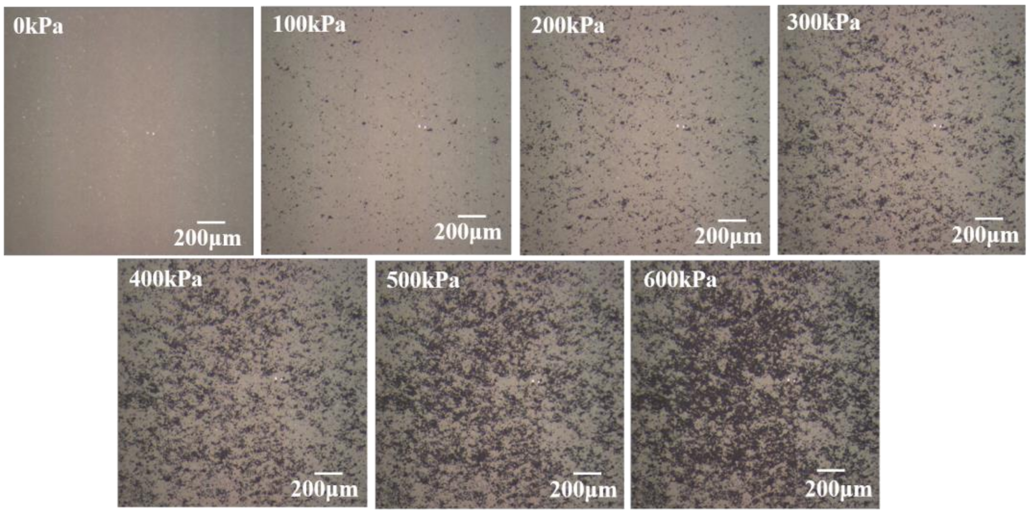

Figure 7. Confocal microscope images showing the increase in the contact area of the elastomer with increasing pressure.

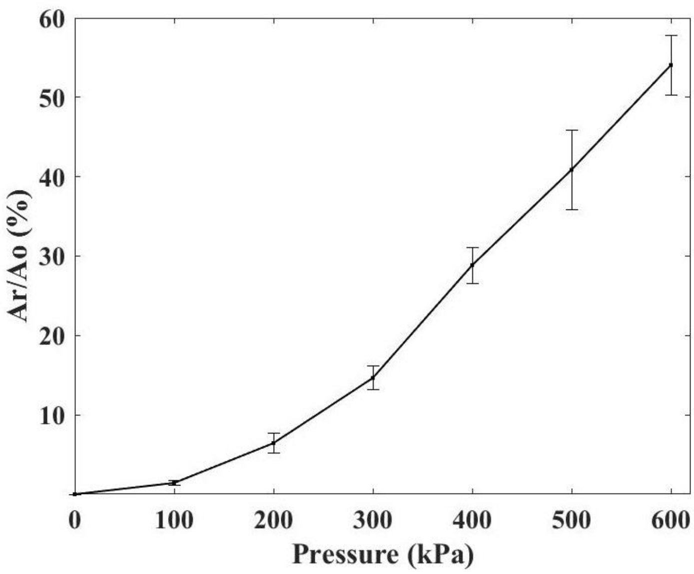

Figure 8. Change in the contact area ratio with increasing pressure.

3.4. Relationship between Conductance of Conductive Elastomer and Change in Contact Area

We considered the relationship between the changes in the contact area of this conductive elastomer and sensor response. Figure 9 shows the result of calculating the value of resistance change with respect to the pressure increase shown in Figure 6 into the conductance. It can be seen that the conductance increases almost linearly as the pressure increases. Using the rate of change in contact area obtained in Figure 8, the contact area when pressure increased was calculated, and from the average value of conductance with respect to pressure increase (Figure 9), the conductance changes with respect to increase in contact area was derived. Figure 10 shows the increase in conductance as the contact area increases. At this time, the correlation coefficient (r) determined from the regression line was 0.964, confirming a strong correlation between contact area and conductance. It is highly likely that the increase in the contact area of the conductive elastomer with the electrode contributes to the increase in conductance (reduction in resistance value).

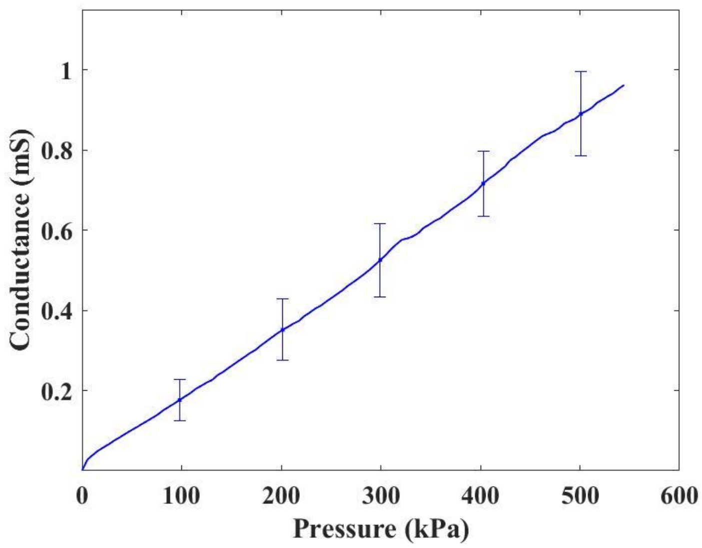

Figure 9. Conductance change with increasing pressure.

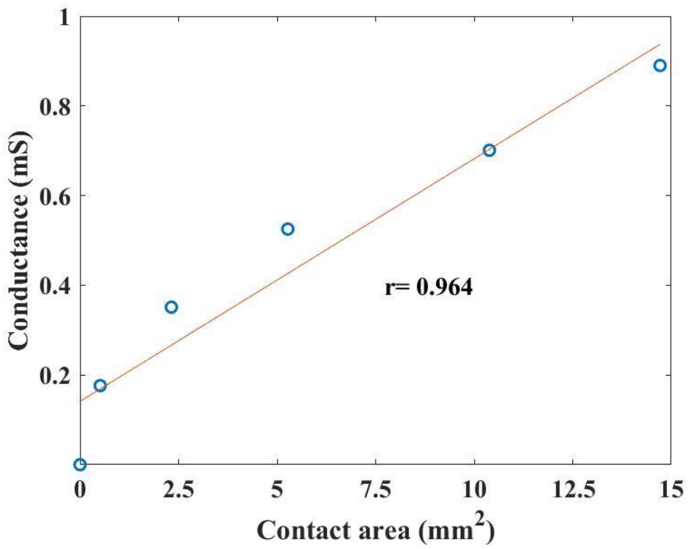

Figure 10. Conductance change in the elastomer with respect to the contact area.

In this conductive elastomer, even when conductive grease was used, internal resistance changes occurred due to an increase in external pressure. In addition to this phenomenon, we also observed changes in the contact surface as the external pressure increased, suggesting that both the changes inside the conductive elastomer and changes in the contact surface may influence the sensor response.

In this study, the correlation between changes in conductance and changes in contact area was confirmed. However, we were unable to clearly demonstrate the relationship between contact area and resistance value. Some reports on contact area measurement explain the color change of the glass surface caused by a polymeric material coming into contact with it. These techniques use binarization to compute the ratio of the contact surface between the glass and polymeric material [22,27–29]. Preliminary research methods are considered effective for observing changes in the contact surface. We also created the compression device, as shown in Figure 3, to photograph the contact surface using a confocal microscope and measured the ratio of the contact surface by binarizing it. Because of this, it is considered that the increase in the contact surface of the elastomer due to the increase in pressure was correctly measured. However, the issue that arose when observing the compressed surface of this elastomer. Among the fillers distributed on the surface of the conductive elastomer used in this research, silicone resin powder is distributed on the elastomer surface, as shown in Figure 4a. This silicone resin powder is not electrically conductive and is distributed over the entire elastomer surface. Furthermore, silicones also contain materials that can interfere with conductivity, such as aluminum oxide particles and silicone elastomer powders. It was possible to determine these by using the SEM images and elemental mapping images. However, it was difficult to distinguish these particles by color and particle size using a microscope. Since these insulating particles are distributed on the surface of the elastomer, they become a factor that prevents the conduction of current even when the elastomer comes into contact with an object. When this conductive elastomer came into contact with glass, the contact surface was observed as black spots, as shown in Figure 7, and the results showed that there was almost no color change within the black spots on the contact surface. Between the black contact surfaces, it was not possible to recognize the difference in color whether silicone resin powder, aluminum oxide particle, or other material was in contact. Among the black spots on the contact surface, if materials other than carbon particles and DENTALL are in contact, there is a possibility that part of the contact surface is a non-conducting contact surface. Because it was not possible to classify such a non-conducting surface under the present observation conditions, it was also infeasible to evaluate the relationship between resistance value change and contact area change using methods other than showing the correlation coefficient. The future challenge lies in creating an experimental environment that can reveal a clear relationship between the resistance value and the contact area that can be obtained when pressure is applied to the elastomer. Additionally, if the state of contact between the elastomer and the electrode affects the sensor response, it is thought that the state of the filler distributed on the elastomer surface, the surface properties of the contacting electrode, and the surface state of the electrode, such as oxide film, also affect the sensor response. It is expected that the sensor response will be improved by examining the usage conditions of the sensor that take into account the phenomena that occur at the interface between these conductive elastomers and the electrodes.

4. Conclusions

We investigated changes in resistance, conductance, and contact surface due to changes in pressure of the conductive elastomer using a commercially available conductive elastomer. By observing the surface and cross-section of the conductive elastomer used in this research using SEM and obtaining elemental mapping, we confirmed that the conductive filler was dispersed throughout the conductive elastomer. When we conducted a pressure test on this conductive elastomer using conductive grease, it was clear that when conductive grease was used, the insulation properties of this conductive elastomer under no load were not due to the conductive network. Additionally, it was found that the resistance value inside the conductive elastomer changed. When we observed the compressed surface of this conductive elastomer, we found that the contact area ratio increased as the pressure increased; when 100 kPa was applied, 1.4% of the conductive elastomer surface was in contact, and when 500 kPa was applied, 40.9% was in contact. The correlation coefficient between contact area and conductance during pressurization was 0.964.

Because the internal resistance of this conductive elastomer is low and the shape of the surface of the conductive elastomer is deformed, it is highly likely that phenomena occurring at the contact interface with the electrode are affecting the sensor response. Many previous studies have argued that changes inside the conductive elastomer composite or changes in the contact surface cause changes in resistance, but it was confirmed that both changes occur in this conductive elastomer. This is a novel result that elucidates the response of the elastomer composite sensor and also provides useful information for determining usage conditions when utilizing these conductive elastomer sensors.

Author Contributions: Conceptualization, T.K., T.M. and T.N.; methodology, T.K.; investigation, T.K.; resources, K.K.; data curation, T.K., Y.T. and S.K.; writing—original draft preparation, T.K.; writing—review and editing, T.M., K.K. and T.N.; supervision, N.C.T.N., K.U., T.M. and T.N.; project administration, K.U. and T.M.; funding acquisition, T.M., K.K. and T.N. All authors have read and agreed to the published version of the manuscript.

Funding: This research was supported in part by A-STEP (Grant Number: JPMJTR201G) from the Japan Science and Technology Agency (JST).

Data Availability Statement: Data sharing is not applicable to this article.

Acknowledgments: We would like to thank Inaba Rubber Co., Ltd, Osaka, Japan. for providing materials and information.

Conflicts of Interest: The authors declare no conflict of interest.

References

1. Cui, J.; Zhang, B.; Duan, J.; Guo, H.; Tang, J. Flexible pressure sensor with Ag wrinkled electrodes based on PDMS substrate. *Sensors* **2016**, *16*, 2131. [CrossRef] [PubMed]
2. Kou, H.; Zhang, L.; Tan, Q.; Liu, G.; Lv, W.; Lu, F.; Dong, H.; Xiong, J. Wireless flexible pressure sensor based on micro-patterned graphene/PDMS composite. *Sens. Actuators A* **2018**, *277*, 150–156. [CrossRef]
3. Li, S.; Dong, K.; Li, R.; Huang, X.; Chen, T.; Xiao, X. Capacitive pressure sensor inlaid a porous dielectric layer of superelastic polydimethylsiloxane in conductive fabrics for detection of human motions. *Sens. Actuators A* **2020**, *312*, 112106. [CrossRef]
4. Wang, F.; Tan, Y.; Peng, H.; Meng, F.; Yao, X. Investigations on the preparation and properties of high-sensitive $BaTiO_3$/MwCNTs/PDMS flexible capacitive pressure sensor. *Mater. Lett.* **2021**, *303*, 130512. [CrossRef]
5. Hwang, J.; Kim, Y.; Yang, H.; Oh, J.H. Fabrication of hierarchically porous structured PDMS composites and their application as a flexible capacitive pressure sensor. *Compos. B Eng.* **2021**, *211*, 108607. [CrossRef]
6. Yin, M.J.; Yin, Z.; Zhang, Y.; Zheng, Q.; Zhang, A.P. Micropatterned elastic ionic polyacrylamide hydrogel for low-voltage capacitive and organic thin-film transistor pressure sensors. *Nano Energy* **2019**, *58*, 96–104. [CrossRef]
7. Wang, T.; Zhang, Y.; Liu, Q.; Cheng, W.; Wang, X.; Pan, L.; Xu, B.; Xu, H. A self-healable, highly stretchable, and solution processable conductive polymer composite for ultrasensitive strain and pressure sensing. *Adv. Funct. Mater.* **2018**, *28*, 1705551. [CrossRef]
8. Zhu, W.B.; Luo, H.S.; Tang, Z.H.; Zhang, H.; Fan, T.; Wang, Y.Y.; Huang, P.; Li, Y.Q.; Fu, S.Y. Ti3C2Tx MXene/Bamboo fiber/PDMS pressure sensor with simultaneous ultrawide linear sensing range, superb environmental stability, and excellent biocompatibility. *ACS Sustain. Chem. Eng.* **2022**, *10*, 3546–3556. [CrossRef]
9. Frenkel, J. On the electrical resistance of contacts between solid conductors. *Phys. Rev.* **1930**, *36*, 1604–1618. [CrossRef]
10. van Beek, L.K.H.; van Pul, B.I.C.F. Internal field emission in carbon black-loaded natural rubber vulcanizates. *J. Appl. Polym. Sci.* **1962**, *6*, 651–655. [CrossRef]
11. Polley, M.H.; Boonstra, B.B.S.T. Carbon blacks for highly conductive rubber. *Rubber Chem. Technol.* **1957**, *30*, 170–179. [CrossRef]
12. Simmons, J.G. Generalized formula for the electric tunnel effect between similar electrodes separated by a thin insulating film. *J. Appl. Phys.* **1963**, *34*, 1793–1803. [CrossRef]
13. Canavese, G.; Stassi, S.; Fallauto, C.; Corbellini, S.; Cauda, V.; Camarchia, V.; Pirola, M.; Pirri, C.F. Piezoresistive flexible composite for robotic tactile applications. *Sens. Actuators A* **2014**, *208*, 1–9. [CrossRef]
14. Lantada, A.D.; Lafont, P.; Sanz, J.L.M.; Munoz-Guijosa, J.M.; Otero, J.E. Quantum tunnelling composites: Characterisation and modelling to promote their applications as sensors. *Sens. Actuators A* **2010**, *164*, 46–57. [CrossRef]
15. Qin, R.; Li, X.; Hu, M.; Shan, G.; Seeram, R.; Yin, M. Preparation of high-performance MXene/PVA-based flexible pressure sensors with adjustable sensitivity and sensing range. *Sens. Actuators A* **2022**, *338*, 113458. [CrossRef]
16. Luheng, W.; Tianhuai, D.; Peng, W. Effects of conductive phase content on critical pressure of carbon black filled silicone rubber composite. *Sens. Actuators A* **2007**, *135*, 587–592. [CrossRef]
17. Wang, L.; Xu, C.; Li, Y. Piezoresistive response to changes in contributive tunneling film network of carbon nanotube/silicone rubber composite under multi-load/unload. *Sens. Actuators A* **2013**, *189*, 45–54. [CrossRef]
18. Hu, S.; Xiang, Y.; Sun, Z.; Fu, X.; Liu, Q.; Lou, D.; Hu, T.; Ping Wong, C.P.; Zhang, R. Highly flexible composite with improved Strain-Sensing performance by adjusting the filler network morphology through a soft magnetic elastomer. *Compos. Part A Appl. Sci. Manuf.* **2022**, *163*, 107188. [CrossRef]
19. Yang, Y.J.; Cheng, M.Y.; Shih, S.C.; Huang, X.H.; Tsao, C.M.; Chang, F.Y.; Fan, K.C. A 32 × 32 temperature and tactile sensing array using PI-copper films. *Int. J. Adv. Manuf. Technol.* **2010**, *46*, 945–956. [CrossRef]
20. Drimus, A.; Kootstra, G.; Bilberg, A.; Kragic, D. Design of a flexible tactile sensor for classification of rigid and deformable objects. *Robot. Auton. Syst.* **2014**, *62*, 3–15. [CrossRef]
21. Cho, C.; Ryuh, Y. Fabrication of flexible tactile force sensor using conductive ink and silicon elastomer. *Sens. Actuators A Phys.* **2016**, *237*, 72–80. [CrossRef]

22. Helseth, L.E. Simple fabrication of a multiwall carbon nanotube–elastomer composite with a rough surface and its application in force sensing. *Microelectron. Eng.* **2018**, *199*, 106–113. [CrossRef]
23. Park, J.; Lee, Y.; Hong, J.; Ha, M.; Do Jung, Y.; Lim, H.; Kim, S.Y.; Ko, H. Giant tunneling piezoresistance of composite elastomers with interlocked microdome arrays for ultrasensitive and multimodal electronic skins. *ACS Nano* **2014**, *8*, 4689–4697. [CrossRef] [PubMed]
24. Tsai, Y.C.; Ma, C.W.; Lin, Y.H.; Yang, Y.J. Development of a large-area 8 × 8 tactile sensing array with high sensitivity. *Sensors Mater* **2017**, *29*, 303–309. [CrossRef]
25. Park, J.; Kim, J.; Hong, J.; Lee, H.; Lee, Y.; Cho, S.; Kim, S.W.; Kim, J.J.; Kim, S.Y.; Ko, H. Tailoring force sensitivity and selectivity by microstructure engineering of multidirectional electronic skins. *NPG Asia Mater.* **2018**, *10*, 163–176. [CrossRef]
26. Wang, G.; Zheng, M.; Liu, M.; Wang, M. Anisotropic Piezoresistive Sensors Made with Magnetically Induced Vertically Aligned Carbon Nanotubes/Polydimethylsiloxane. *ACS Appl. Mater. Interfaces* **2023**. [CrossRef]
27. Ovcharenko, A.; Halperin, G.; Etsion, I. In situ and real-time optical investigation of junction growth in spherical elastic-plastic contact. *Wear* **2008**, *264*, 1043–1050. [CrossRef]
28. Prevost, A.; Scheibert, J.; Debrégeas, G. Probing the micromechanics of a multi-contact interface at the onset of frictional sliding. *Eur. Phys. J. E Soft Matter* **2013**, *36*, 17. [CrossRef]
29. Sahli, R.; Pallares, G.; Ducottet, C.; Ben Ali, I.E.; Al Akhrass, S.; Guibert, M.; Scheibert, J. Evolution of real contact area under shear and the value of static friction of soft materials. *Proc. Natl Acad. Sci. USA* **2018**, *115*, 471–476. [CrossRef]
30. Pohtongkam, S.; Srinonchat, J. Tactile object recognition for humanoid robots using new designed piezoresistive tactile sensor and DCNN. *Sensors* **2021**, *21*, 6024. [CrossRef]
31. Ramalingame, R.; Hu, Z.; Gerlach, C.; Rajendran, D.; Zubkova, T.; Baumann, R.; Kanoun, O. Flexible piezoresistive sensor matrix based on a carbon nanotube PDMS composite for dynamic pressure distribution measurement. *J. Sens. Sens. Syst.* **2019**, *8*, 1–7. [CrossRef]
32. Rahmani, P.; Shojaei, A. A review on the features, performance and potential applications of hydrogel-based wearable strain/pressure sensors. *Adv. Colloid Interface Sci.* **2021**, *298*, 102553. [CrossRef] [PubMed]
33. Shimojo, M.; Namiki, A.; Ishikawa, M.; Makino, R.; Mabuchi, K. Rubber with electrical-wires stitched method. *October* **2004**, *4*, 589–596.
34. Teshigawara, S.; Tsutsumi, T.; Suzuki, Y.; Shimojo, M. High speed and high sensitivity slip sensor for dexterous grasping. *J. Robot. Mechatron.* **2012**, *24*, 298–310. [CrossRef]
35. Wang, Y.; Xi, K.; Mei, D.; Liang, G.; Chen, Z. A flexible tactile sensor array based on pressure conductive rubber for contact force measurement and slip detection. *J. Robot. Mechatron.* **2016**, *28*, 378–385. [CrossRef]